The Journal of Immunology

Unique Structural Determinants for Stat3 Recruitment and Activation by the Granulocyte Colony-Stimulating Factor Receptor at Phosphotyrosine Ligands 704 and 744

Huang Shao, Xuejun Xu, Naijie Jing and David J. Tweardy

J Immunol 2006; 176:2933-2941; ;
doi: 10.4049/jimmunol.176.5.2933
http://www.jimmunol.org/content/176/5/2933

The Journal of Immunology is published twice each month by
The American Association of Immunologists, Inc.,
1451 Rockville Pike, Suite 650, Rockville, MD 20852

Print ISSN: 0022-1767 Online ISSN: 1550-6606.

Unique Structural Determinants for Stat3 Recruitment and Activation by the Granulocyte Colony-Stimulating Factor Receptor at Phosphotyrosine Ligands 704 and 744[1]

Huang Shao, Xuejun Xu, Naijie Jing, and David J. Tweardy[2]

G-CSFR cytoplasmic tyrosine (Y) residues (Y704, Y729, Y744, and Y764) become phosphorylated upon ligand binding and recruit specific Src homology 2 domain-containing proteins that link to distinct yet overlapping programs for myeloid cell survival, differentiation, proliferation, and activation. The structural basis for recruitment specificity is poorly understood but could be exploited to selectively target deleterious G-CSFR-mediated signaling events such as aberrant Stat3 activation demonstrated in a subset of acute myeloid leukemia patients with poor prognosis. Recombinant Stat3 bound to G-CSFR phosphotyrosine peptide ligands pY^{704}VLQ and pY^{744}LRC with similar kinetics. Testing of three models for Stat3 Src homology 2-pY ligand binding in vitro and in vivo revealed unique determinants for Stat3 recruitment and activation by the G-CSFR, the side chain of Stat3 R609, which interacts with the pY ligand phosphate group, and the peptide amide hydrogen of E638, which bonds with oxygen/sulfur within the + 3 Q/C side chain of the pY ligand when it assumes a β turn. Thus, our findings identify for the first time the structural basis for recruitment and activation of Stat3 by the G-CSFR and reveal unique features of this interaction that can be exploited to target Stat3 activation for the treatment of a subset of acute myeloid leukemia patients. *The Journal of Immunology,* **2006, 176: 2933–2941.**

Signal transducer and activator of transcription 3 is a latent transcription factor involved in cell growth, differentiation, and apoptosis that is activated by a variety of cytokine and growth factor receptors, including G-CSF (1–3). Studies to assess the physiologic role of Stat3 activation by G-CSF in which wild-type and dominant-negative Stat3 constructs were overexpressed in myeloid cell lines and murine bone marrow progenitor cells supported the concept that the role of Stat3 in G-CSFR signaling in normal myeloid progenitor cells is to promote cell survival and to help direct myeloid maturation (4–9). Studies examining oncogenic signaling pathways active at a single-cell level in acute myeloid leukemia (AML)[3] demonstrated that Stat3 activation by G-CSF was associated with relapse following initial chemotherapy in the subset of AML cells containing Flt3 with an internal duplication (10).

The G-CSFR is a member of the type I cytokine receptor family (11). Ligand-induced dimerization of the G-CSFR results in activation of receptor-associated protein tyrosine kinases (PTK) most notably those of the Jak kinase family (1, 12–14). Activation of receptor-associated PTK results in phosphorylation of tyrosine (Y) residues located within the C-terminal end of the cytoplasmic domain of the receptor (Y704, Y729, Y744, and Y764 in the human receptor; Y703, Y728, Y743, and Y763 in the murine receptor) and recruitment of Src homology 2 (SH2)-containing proteins to these sites, including Shc to Y764 (15, 16), SHP-2 to Y704 and Y764 (6), PI3K to Y704 (17), SOCS-3 to Y704 and Y729 (18), Grb2 and the adapter protein, 3BP2, to Y764 (6, 16), and Stat3 to Y704 and Y744 (19, 20). Following its recruitment to Y704 and Y744, Stat3 is phosphorylated on Tyr^{705} by receptor-associated Jak kinase family members, leading to dimerization mediated by reciprocal SH2-pY705 motif interactions, nuclear translocation, and binding to specific DNA elements.

The preference of SH2 domain binding to specific phosphotyrosine (pY) peptide ligands was shown to map to the three residues immediately C-terminal to the pY (21, 22). G-CSFR Y704 is followed at the + 3 position by the polar amino acid residue Q, thereby conforming to the consensus Stat3 SH2-binding motif, YxxQ (23, 24). G-CSFR Y744 is followed at the + 3 position by the polar residue C. Among the group of SH2-containing proteins that bind pY motifs within the G-CSFR, with the exception of Grb2 (25), the structural basis for their pY binding preferences is poorly understood. The preference for Stat3 SH2 for pY peptide ligands containing Q (or the polar residue C) at the + 3 position is unique among SH2 domains. Consequently, structural information regarding Stat3 SH2 binding to its preferred pY ligands might be expected to yield information that could be exploited to specifically target Stat3 recruitment and activation.

Although the structure of Stat3 SH2 bound to pY peptide ligand has not been solved, the structure of Stat3β dimers, including their SH2 domains, is available bound to DNA (26). Although the authors were able to conclude that Stat3 SH2 shares features of other SH2 domains, the structure of the SH2 domain obtained did not clarify the molecular basis for the Stat3 SH2-pY peptide ligand interaction, especially the preference of Stat3 SH2 for binding to pY peptide ligands with Q at the + 3 position. Two models have been proposed to explain this preference (19, 27); both assume an extended configuration for the pY peptide ligand and two pockets—one, a positively charged pocket, that interacts with the pY

Section of Infectious Diseases, Department of Medicine, Baylor College of Medicine, Houston, TX 77030

Received for publication August 17, 2005. Accepted for publication November 22, 2005.

The costs of publication of this article were defrayed in part by the payment of page charges. This article must therefore be hereby marked *advertisement* in accordance with 18 U.S.C. Section 1734 solely to indicate this fact.

[1] This work is supported, in part, by National Institutes of Health R01 Grant CA86430.

[2] Address correspondence and reprint requests to Dr. David J. Tweardy, Section of Infectious Diseases, Baylor College of Medicine, One Baylor Plaza, BCM 286, Room 1319, Houston, TX 77030. E-mail address: dtweardy@bcm.edu

[3] Abbreviations used in this paper: AML, acute myeloid leukemia; PTK, protein tyrosine kinase; SH2, Src homology 2; EGFR, epidermal growth factor receptor; pStat3, phosphorylated Stat3.

0022-1767/06/$02.00

residue and the other, a hydrophilic pocket, that interacts with the + 3 Q.

Using wild-type and mutated Stat3 in peptide immunoblot and mirror resonance affinity analyses with Y704- and Y744-derived peptides, we demonstrated that binding of the pY residue within the peptide to Stat3 SH2 requires interaction of the phosphate group with the side chains of K591 and R609 within the Stat3 SH2. Furthermore, binding of Stat3 SH2 to pYxxQ/C-containing peptides does not require the side chains of E638, Y640, and Y657 or Y657, C687, S691, and Q692 proposed to form pocket 2 in the Chakraborty et al. (19) and Hemmann et al. (27) models, respectively. Rather, our affinity analysis coupled with computer modeling supports a model in which the pY ligand has a β turn, which allows the oxygen on the side chain of the + 3 Q or the sulfur on the side chain of the + 3 C to hydrogen bond with the amide hydrogen within the peptide backbone of Stat3 at E638. Coexpression of full-length G-CSFR with either wild-type or mutant Stat3 cDNA constructs in vivo indicated that the side chain of R609 and the amide hydrogen of E638 within the Stat3 SH2 domain make major contributions to Stat3 recruitment and activation, while the side chain of K591 makes a less important contribution. These findings outline for the first time the structural requirements for the recruitment and activation of Stat3 by the G-CSFR, which may be exploited for targeting G-CSF-mediated Stat3 activation for the treatment of a subset of AML patients in whom Stat3 activation is associated with poor prognosis using current regimens.

Materials and Methods

Site-directed mutagenesis of Stat3

The human Stat3α cDNA was a gift from Dr. R. Van de Groot (28). A *Hin*dIII/*Xho*I cDNA fragment encoding full-length Stat3 was subcloned into the baculovirus expression vector, pFastBac1 (Invitrogen Life Technologies) that placed a 6-histidine tag onto the N terminus of Stat3. Single or combination mutations were generated using the Quikchange site-directed mutagenesis kit (Stratagene) to target amino acid residues within the Stat3 SH2 domain implicated in models of Stat3 SH2-phosphotyrosine binding (K591L, R609L, E638P, E638L, Y640F, Y657F, C687A, S691A, and Q692L; see Fig. 1). The sequence of each construct was verified by sequencing analysis.

Expression and purification of Stat3 proteins

Wild-type and mutated Stat3 plasmids were used to transform DH10Bac-competent cells, which contain a bacmid with a miniattTn7 target site and helper plasmid. Recombinant bacmids were prepared and used to infect Sf9 cells. Sf9 cells (3×10^6 cells/ml) were infected with Stat3 recombinant virus at a multiplicity of infection of 0.05 and harvested after 3-day culture. Cells (6×10^8) were suspended in 12-ml precooled lysis buffer (20 mM Tris-HCl (pH 8.0), 0.5M NaCl, 10% glycerol, 1 mM PMSF, 10 μg/ml leupeptin, 1 μg/ml aprotinin, and 10 mM imidazole) and lysed by ultrasonication on ice. Lysates were centrifuged at $15,000 \times g$ for 30 min at 4°C, and the supernatant was incubated with Ni-NTA agarose (Qiagen) at 4°C for 1 h. The Ni-NTA resin was washed twice with 4 volumes of wash buffer (20 mM Tris-HCl (pH 8.0), 0.5 M NaCl, 10% glycerol, 1 mM PMSF, 10 μg/ml leupeptin, 1 μg/ml aprotinin, and 20 mM imidazole) to remove unbound proteins. Stat3 was eluted from the Ni-NTA resin with elution buffer (20 mM Tris-HCl (pH 8.0), 0.5M NaCl, 10%glycerol, 1 mM PMSF, 10 μg/ml leupeptin, 1 μg/ml aprotinin, and 250 mM imidazole). Purified proteins were dialyzed against 10 mM PBS at 4°C and stored at −80°C.

Peptide synthesis

The peptides listed in Table I were synthesized in the Baylor College of Medicine Protein Core Facility on an Applied Biosystems Model 433A peptide synthesizer using standard 9-fluorenylmethoxycarbonyl amino acid chemistry. Seventy percent of the peptide reaction mix was biotinylated at the N terminus, while the peptide remained on the resin using d-Biotin-LC (AnaSpec). All peptides were purified using reverse-phase HPLC and were ≥95% pure.

Table I. *Tyrosine phosphorylated and nonphosphorylated peptides synthesized based on the G-CSFR sequence*

Peptide	Amino Acid Sequence
Y704	TLVQTYVLQGDP
pY704	TLVQTpYVLQGDP
pY729	SDQVLpYGQLLGS
Y744	PGPGHYLRCDST
pY744	PGPGHpYLRCDST
pY764	PSPLSpYENLTFQ

Phosphopeptide affinity immunoblot analysis

NeutrAvidin agarose (40 μl; Pierce) was incubated with 10 μg of biotinylated peptide in 300 μl of buffer A (20 mM HEPES (pH 7.5), 20 mM NaF, 1 mM Na_3VO_4, 1 mM $Na_4P_2O_7$, 1 mM EDTA, 1 mM EGTA, 20% glycerol, 0.05% Nonidet P-40, 1 mM DTT, 1 μg/ml leupeptin, 1 μg/ml aprotinin, 0.5 mM PMSF, and 100 mM NaCl) at 4°C for 2 h and washed with buffer A three times. The NeutrAvidin-peptide complex was then mixed with His-tagged Stat3 protein (5 μg) in 1 ml of buffer A (without NaCl and Nonidet P-40) at 4°C for 2 h and washed thoroughly. Bound proteins were separated and immunoblotted using Stat3 mAb as described previously (29).

Mirror resonance affinity assay

Kinetics experiments were performed using an Iasys Auto$^+$ resonance mirror biosensor (Affinity Sensor) as described previously (30). Briefly, a two-welled cuvette coated on the bottom of each well with biotin was purchased from Affinity Sensor and prepared for immobilization of biotinylated peptides by coating each surface with 0.04 mg/ml NeutrAvidin (Pierce) and washing with PBST (20 mM sodium phosphate and 0.05% Tween 20). Biotinylated peptide (5 μg) was added into each well, and change in arc seconds was monitored simultaneously in both wells using the biosensor until stable, followed by washing with PBST. Real-time binding of Stat3 was conducted at 25°C at a stir setting of 70 for 10 min starting at the lowest concentration of Stat3. The wells were washed out with three changes of 60 μl of PBST, and dissociation was allowed to proceed for 5 min. Each well bottom was regenerated by washing with 50 μl of 100 mM formic acid for 2 min and equilibrated with PBST for the next round of association assay. Data were collected automatically and analyzed with the FASTplot and GraFit software (31).

Coexpression of G-CSFR and Stat3 in 293T cells

*Hin*dIII/*Xho*I cDNA fragments encoding His-tagged wild-type and mutant Stat3 were subcloned into pcDNA3.1(−) (Invitrogen Life Technologies). The full-length human G-CSFR cDNA was a gift from Dr. S. F. Ziegler (Department of Immunology, University of Washington, Seattle, WA) (32). Both the G-CSFR and Stat3 vectors were cotransfected using Fugene6 (Roche) into 293T cells. These cells have been used previously to perform reporter assays to assess levels of Stat3 activation downstream of the human G-CSFR (33). Forty-eight hours after transfection, cells were starved for 6 h and stimulated with 100 ng/ml G-CSF (R&D Systems) for 15 min. For immunoprecipitation, cells were placed in lysis buffer (50 mM Tris-HCl, 150 mM NaCl, 1% Nonidet P-40, 1 mM EDTA, 0.25% sodium deoxycholate, 1 mM PMSF, 10 μg/ml leupeptin, and 10 μg/ml aprotinin) and sonicated. Lysate supernatants were incubated with anti-G-CSFR Ab (CD114; RDI) at 4°C for 1 h, followed by incubation with protein G-Sepharose (Sigma-Aldrich) for 2 h. Immunoprecipitates were washed five times with lysis buffer then boiled for 5 min in SDS-PAGE sample buffer. For Ni-His-tagged protein pull-down assay, cells were placed in cell suspension buffer (20 mM Tris-HCl (pH 8.0), 0.5M NaCl, 10% glycerol, 1 mM PMSF, 10 μg/ml leupeptin, 1 μg/ml aprotinin, and 10 mM imidazole) and lysed by ultrasonication on ice. The supernatant was incubated with Ni-NTA agarose (Qiagen) at 4°C for 2 h. The Ni-NTA agarose was washed five times with cell suspension buffer containing 20 mM imidazole to remove unbound proteins then boiled for 5 min in SDS-PAGE sample buffer. Immunoprecipitates and Ni-NTA pulldowns were separated on SDS-PAGE gels and transferred to polyvinylidene difluoride membranes. G-CSFR was detected by anti-human G-CSFR Ab (R&D Systems). Total Stat3 was detected as described above; Y705 phosphorylated Stat3 was detected using Abs purchased from BD Transduction Laboratories or Cell Signaling Technology.

Results

Stat3 binds directly to G-CSFR Y704 and Y744 phosphododecapeptides

Previous studies by us (19) and others (34) using the M1 cell line containing wild-type G-CSFR constructs and constructs containing Y-to-F mutants at single and multiple Y residues within its cytoplasmic domain indicated that G-CSF-mediated Stat3 activation and differentiation mapped to both Y704 and Y744. In addition, Stat3 destabilization and peptide affinity studies using phosphododecapeptides based upon each of the four pY sites within the G-CSFR indicated that only Y704 and Y744 were able to destabilize Stat3 dimers and to affinity purify Stat3 from whole cell extracts (19). Ward et al. (6) confirmed the Stat3 destabilization results using phosphopeptides that were nine residues in length and based on the four pY sites within the murine G-CSFR; they also demonstrated direct binding of a GST-Stat3 SH2 domain fusion protein to the phosphorylated cytoplasmic domain of the human G-CSFR (6), which indicated that the interaction was mediated through the Stat3 SH2 domain. To further establish that the Stat3 SH2 domain binds directly to G-CSFR at Y704 and Y744 sites, we generated recombinant human Stat3 protein with a His tag added at the N terminus to aid in purification; we previously demonstrated that this modification did not interfere with binding of wild-type Stat3 to native full-length, activated epidermal growth factor receptor (EGFR) or to EGFR-derived phosphododecapeptides (29). Recombinant wild-type Stat3 protein was expressed in Sf9 insect cells and purified using Ni-NTA resin (Fig. 1*C*).

Purified Stat3 was incubated with phosphododecapeptides based on each of the four G-CSFR Y residues (Table I) in pull-down assays (Figs. 2*A*). Immunoblotting for Stat3 demonstrated a prominent Stat3 band in pull-down assays using Y704 and Y744 phosphododecapeptide. Neither of the other two G-CSFR phosphododecapeptides bound purified Stat3 above control level. The ability of both Y704 and Y744 dodecapeptides to bind purified Stat3 depended on the tyrosine being phosphorylated.

To obtain quantitative kinetic information about the binding of Stat3 to G-CSFR Y704 and Y744, including association rates (k_{ass}), disassociation rates (k_{diss}), and dissociation equilibrium constants (K_D), we performed real-time affinity measurements using a mirror resonance biosensor. The biosensor exploits surface plasmon resonance to measure in real time the alteration in the angle of a laser light reflected from a surface on which binding events are occurring. Biotinylated peptides were immobilized onto the bottom surface of cuvette wells precoated with NeutrAvidin. The interaction of peptides with Stat3 added at different concentrations was measured in real time as altered deflection of a laser light striking the bottom surface of the cuvette; the alterations in the deflection angle measured in arc seconds were analyzed with GraFit software. Mirror resonance analysis (Fig. 2, *B* and *C*, and Table II) demonstrated that Stat3 bound to phosphododecapeptide Y704 with a K_D of 0.703 μM, similar to phosphododecapeptide Y744, which demonstrated a K_D of 0.95 μM. The slightly lower K_D for Y704 vs Y744 is attributable to a faster association rate of Stat3 binding to this phosphododecapeptide.

The side chains of K591 and R609 within pocket 1 of Stat3, but not the side chains of amino acid residues within pocket 2, are essential for Stat3 binding to Y704 and Y744 phosphododecapeptides

We (19) previously proposed a two-pocket model for the binding of G-CSFR Y704 and Y744 phosphopeptide ligands by the Stat3 SH2 domain (Fig. 1*A*) that was distinct yet had overlapping features with that proposed by Hemmann et al. (27) for binding of Stat3 SH2 to pY ligands within the IL-6Rβ (gp130). Both models assumed the peptide ligand was in an extended configuration. In our model, the phosphotyrosine residue interacts with a positively charged pocket (pocket 1) within the SH2 domain formed by the side chains of K591 and R609. The + 3 Q/C was predicted to interact with a hydrophilic pocket (pocket 2) formed by the side chains of E638, Y640, and Y657. In the Hemmann model, the phosphotyrosine was predicted to interact with the side chain of R609 (pocket 1) and the + 3 Q with the side chains of Y657, C687, S691, and Q692 (pocket 2).

To test each of the two models proposed, we generated Stat3 proteins in which mutations were introduced to alter side chains from charged or polar to nonpolar within amino acid residues predicted in each model to be critical for Stat3 binding (Fig. 1*B*). The recombinant Stat3 proteins were expressed in Sf9 insect cells and purified to equivalent levels using Ni-NTA resin (Fig. 1*C*). Peptide affinity immunoblot studies using Stat3-3M to test the pocket 2 component of the Chakraborty model demonstrated levels of Stat3-3M bound to Y704 and Y744 phosphododecapeptides similar to wild-type Stat3 (Fig. 2*A*). Peptide affinity immunoblot studies using Stat3-4M to test the pocket 2 component of the Hemmann model also demonstrated levels of binding of Stat3-4M bound to Y704 and Y744 phosphododecapeptides equivalent to wild-type Stat3 (Fig. 2*A*). Furthermore, Stat3-6M, in which all six amino acid residues predicted by both models to form pocket 2 were mutated, bound both phosphododecapeptides at levels similar to wild-type Stat3. These results do not support either model for Stat3 SH2 binding to + 3 Q/C within phosphopeptide ligands.

To test the pocket 1 component of the two models and to ensure that our peptide pull-down system was sufficiently sensitive to detect reduced binding of Stat3 containing mutations in pocket 2, we added either K591L or R609L to the 3M mutant to generate Stat3-3M+K591L and Stat3-3M+R609L. Addition of either mutation resulted in elimination of binding to both Y704 and Y744 phosphododecapeptides, indicating that each of the side chains of K591 and R609 contribute to binding of the phosphotyrosine.

To confirm these findings and to determine whether introduction of the pocket 2 mutations resulted in subtle alterations in kinetics of binding undetectable using phosphopeptide affinity immunoblot analysis, we performed mirror resonance affinity assays using phosphorylated and nonphosphorylated Y704 and Y744 dodecapeptides (Fig. 2, *B* and *C*, and Table II). Review of the real-time mirror resonance affinity curves (Fig. 2, *B* and *C*) and kinetic analysis (Table II) revealed low or undetectable binding of Stat3-3M+R609L and Stat3-3M+K591L, respectively, to Y704 and Y744 phosphododecapeptide, confirming the results of peptide immunoblot analysis. The pocket 2 mutant Stat3 protein, Stat3-3M, demonstrated k_{ass}, k_{diss}, and K_D values for binding to Y744 phosphododecapeptide indistinguishable from wild-type Stat3 binding to this peptide confirming the peptide immunoblot analysis. The kinetic results of Stat3-3M binding to Y704 revealed a K_D of 1.21 μM, which was increased 72% compared with wild-type Stat3 and attributable to a slower k_{ass}. These results indicate that Stat3 SH2 binding to the + 3 C within Y744 does not require any of the side chains predicted in either of the proposed models, while those side chains proposed in the Chakraborty model make a contribution, albeit small, to binding of Stat3 SH2 to + 3 Q within Y704.

Computational modeling of Stat3 SH2 binding to + 3 Q within Y704 phosphododecapeptide

There is no structural information yet available regarding the binding of any SH2 domain-containing protein to any of the pY motifs within the G-CSFR that could be used to establish a new model for the Stat3 SH2-G-CSFR pY interaction. Consequently, we sought

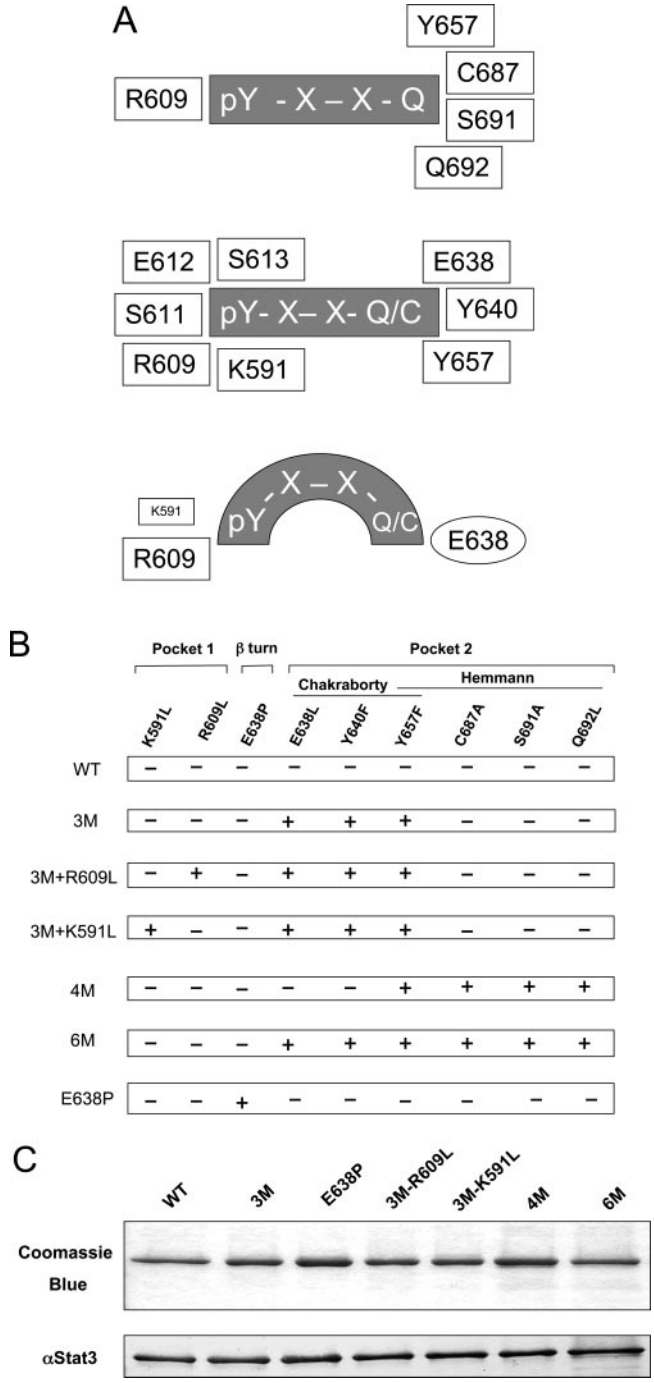

FIGURE 1. Models of Stat3 SH2-phosphotyrosine binding and Stat3 proteins generated to test them. *A*, Schematic representation of three models of Stat3 SH2 binding to pYxxQ/C peptide ligands proposed by Hemmann et al. (*top panel*), Chakraborty et al. (*middle panel*), and by us (*bottom panel*). The first two models assume the peptide is in an extended confirmation, while the model proposed by us in this article assumes the peptide has a β turn. Each model proposes that there are two pockets within the Stat3 SH2 domain. The phosphotyrosine (pY) interacts with a positively charged pocket formed by the side chain(s) of R609 (Hemmann et al. (27)) or by K591 and R609 (Chakraborty et al. (19) and Shao et al. (35)), while pY + 3 Q/C interacts with a hydrophilic pocket within the SH2 domain formed by the side chains of Y657, C687, S691, and Q692 (Hemmann et al.) or E638, Y640, and Y657 (Chakraborty et al.) or with the peptide amide hydrogen of E638 (Shao et al.). Amino acid residues within rectangles indicate that the interaction is with the residue side chain, while residues within ovals indicate that the interaction is with the peptide backbone. *B*, Mutations were introduced at the amino acid residues indicated (+) to generate a panel of wild-type and mutant Stat3 proteins. *C*, Wild-type and mutant Stat3 proteins, each with an N-terminal His-tag, were expressed in SF9 insect cells and affinity purified using Ni-NTA agarose. The proteins were separated by SDS-PAGE, and the gel was stained with Coomassie blue (*top panel*) or immunoblotted using Stat3 mAb (*bottom panel*).

surrogate structures that could be used for computational modeling. We previously demonstrated that Stat3 binds directly to the EGFR within regions of the receptor containing Y1068 and Y1086 (35). The YxxQ motif is contained within both of these regions; each region also contains the consensus motif for Grb2 binding YxNx. The structure of the Y1068 phosphopentapeptide (EpYINQ) is available from its crystal structure bound by Grb2 (36) (PDB code 1ZFP). The structure of Stat3 from W580 to L670 was obtained from the crystal structure of Stat3β homodimer bound to DNA (26) (PDB code 1BG1). These structures were used to generate a new and more robust model for Stat3 SH2 binding to + 3 Q/C by computational modeling of the interaction and identification of the interaction with the lowest energy. All energy minimization calculations were conducted under an AMBER force field by using the DISCOVER/Insight II program. A total of 300 steps of conjugate gradient energy minimization was performed following rigid hand-docking to fit the pY of the EpYINQ peptide into the binding pocket comprised of residues K591 and R609 taking into consideration Van der Waals and Coulomb forces. The complex formed between Stat3-SH2 and EpYINQ with the lowest energy (Fig. 3*A*) had a total binding energy of −478.8 Kcal/mol. This computational result predicted that the major binding energy for this binding configuration comes from a hydrogen bond interaction involving oxygen within the + 3 Q side chain and the peptide amide hydrogen at E638 located within a loop region of Stat3 SH2. Replacement of the EGFR pentapeptide EpYINQ with the G-CSFR Y704-based pentapeptide TpYVLQ did not change the length or angle of this hydrogen bond (Fig. 3*B*).

To test the contribution of the E638 amide hydrogen to binding to G-CSFR Y704 and Y744 phosphododecapeptide, we generated Stat3-E638P by site-directed mutagenesis, which eliminated the amide hydrogen donor predicted to bind with oxygen within the + 3 Q side chain. We had shown previously that introduction into Stat3 of the E638P mutation did not alter secondary structure in computer modeling simulations or when recombinant protein was expressed and purified from Sf9 cells and examined directly by CD analysis (35). Peptide affinity immunoblot assays using recombinant Stat3-E638P (Fig. 1*C*) demonstrated no binding of Stat3-E638P to any of the G-CSFR-derived peptides tested, including Y704 and Y744 phosphododecapeptides (Fig. 2*A*); mirror resonance affinity studies (Fig. 2, *B* and *C*) confirmed these findings. These results strongly support an important role for the E638 amide hydrogen of Stat3 in binding of the + 3 Q within Y704 phosphododecapeptide and the + 3 C within Y744 phosphododecapeptide.

The side chain of amino acid residue R609 and the amide hydrogen of residue E638 within the Stat3 SH2 domain are important for binding and activation of Stat3 by the full-length G-CSFR in vivo

To determine whether the side chains of amino acid residues K591 and R609 and the amide hydrogen of residue E638 within the Stat3 SH2 domain are important for binding of Stat3 to full-length G-CSFR, we compared levels of wild-type and mutant Stat3 within immunoprecipitates of phosphorylated G-CSFR. G-CSFR was immunoprecipitated from G-CSF-stimulated 293T cells cotransfected with full-length G-CSFR cDNA and either wild-type or mutant Stat3 cDNA constructs (Fig. 4*A*). Equivalent levels of total and

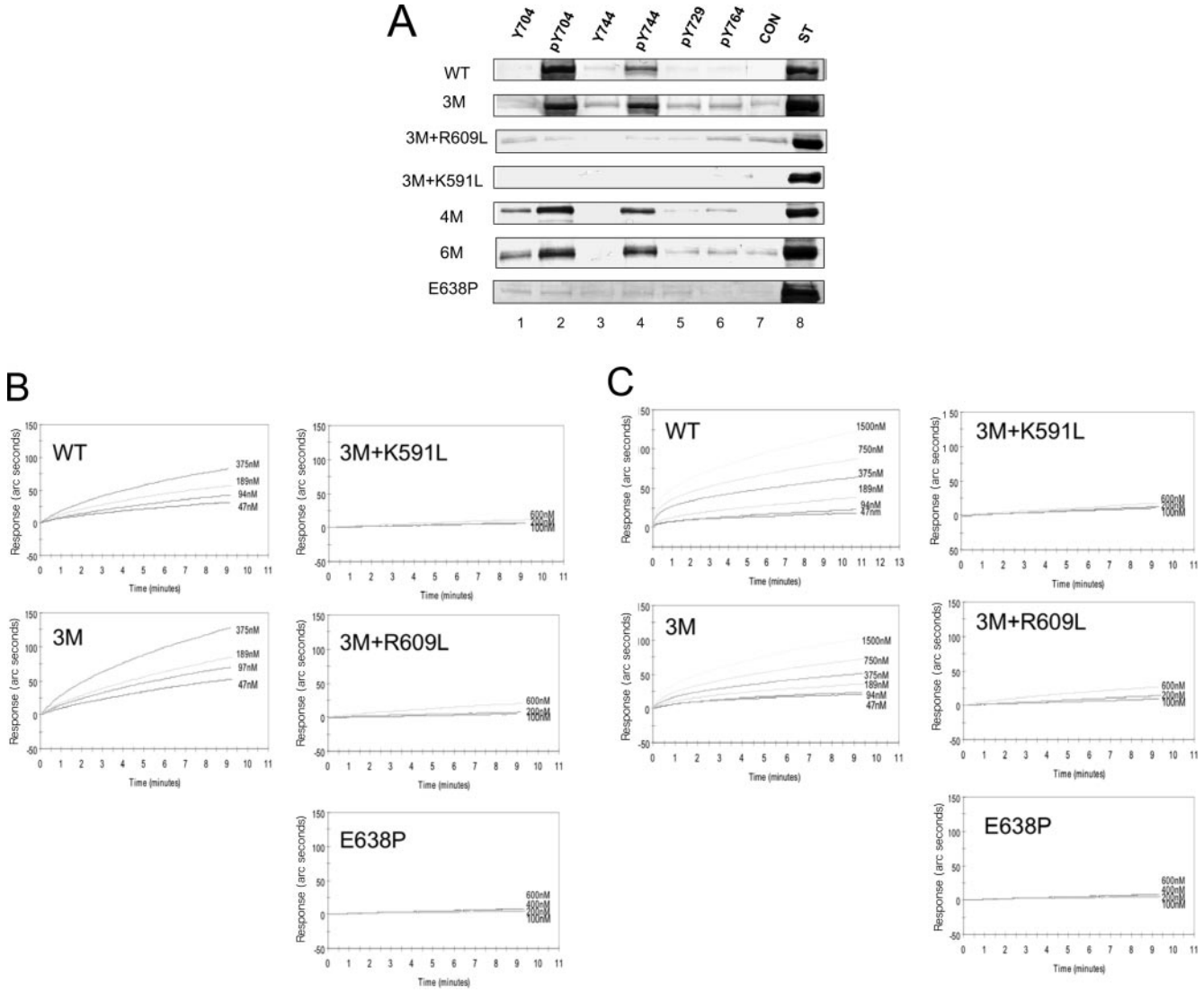

FIGURE 2. Requirement for the side chains of K591 and R609 and the peptide amide hydrogen of E638, but not the side chains of any of the proposed pocket 2 residues, for Stat3 SH2 binding to Y704 and Y744 phosphododecapeptides. *A*, NeutrAvidin agarose was incubated with the indicated biotinylated peptides (see Table I for sequence) or no peptide (CON) as control, washed thoroughly, and mixed with identical amounts of wild-type or mutant Stat3 proteins as indicated. Bound proteins were separated by SDS-PAGE and immunoblotted using Stat3 mAb. *Lane ST* represents purified wild-type Stat3 (0.6 μg) loaded directly onto the gel as positive control. Mirror resonance affinity assay. Cells of a biotin-coated cuvette pretreated with saturating amounts of NeutrAvidin were pretreated with biotinylated phosphopeptide based on Y704 (*B*) or biotinylated phosphopeptide based on Y744 (*C*). Wild-type or mutated Stat3 protein was added in the concentrations indicated, and mirror resonance measurements were recorded continuously for 10 min as shown.

Y705-phosphorylated wild-type Stat3, Stat3-3M, and Stat3-6M protein were found within G-CSFR immunoprecipitates (Fig. 4*A*, *lanes 1–3*) as predicted from the peptide affinity results. In contrast, levels of total Stat3-E638P (Fig. 4*A*, *lane 4*), Stat3-3M-R609L (Fig. 4*A*, *lane 5*), and Stat3–3M-K591L present within G-CSFR immunoprecipitates were reduced by 40–50% compared with wild-type Stat3. Of special note, levels of Y705-phosphorylated Stat3 (pStat3) proteins within G-CSFR immunoprecipitates were either undetectable (Stat3-E638P and Stat3-3M-R609L) or reduced 70–80% (Stat3-3M-K591L). To determine the effects of reduced recruitment to the G-CSFR of the mutated Stat3 proteins on their activation, we examined levels of pStat3 within the lysates of cotransfected cells (Fig. 4*B*) and following Ni-NTA agarose affinity purification of Stat3 (Fig. 4*C*). Levels of pStat3 were similar in lysates cotransfected with G-CSFR and wild-type Stat3, Stat3-3M, or Stat3-6M (Fig. 4*C*, *lanes 1–3*). In contrast, levels of pStat3 were reduced by $\geq$50% in cells transfected with Stat3-E638P (Fig. 4*C*, *lane 4*) and were almost completely absent in cells transfected with Stat3-3M-R609L (Fig. 4*C*, *lane 5*). In contrast, the level of pStat3 in cells transfected with Stat3-3M-K591L (Fig. 4*C*, *lane 6*) were reduced only slightly compared with pStat3 levels in cells transfected with Stat3-3M or wild-type Stat3 (Fig. 4*C*, *lanes 1* and *2*). These findings confirm and extend the Y704 and Y744 phosphododecapeptide binding results and indicate that none of the residue side chains proposed previously by Chakraborty et al. (19) or Hemmann et al. (27) contribute to Stat3 recruitment and activation by the G-CSFR; rather, the side chain of R609 and the amide hydrogen of E638 make major contributions to Stat3 recruitment and activation by the G-CSFR in vivo, while the side chain of K591 makes a minor contribution to these processes.

Discussion

We used recombinant Stat3 and phosphododecapeptides encompassing each of the four Y residues within the cytoplasmic domain of the G-CSFR in peptide pull-down and mirror resonance biosensor assays to establish that Stat3 is capable of binding directly

Table II. *Kinetics of wild-type and mutant Stat3 binding to Y704 and Y744 phosphododecapeptides (PDP) determined by mirror resonance biosensor analysis*

PDP	Stat3	k_{ass} ($M^{-1}s^{-1}$)[a]	k_{diss} (ms^{-1})[b]	K_D (μM)[c]
704	WT	2298	1.6	0.703
	3M	1503 ± 208[d]	1.9 ± 0.3	1.21 ± 0.01
744	WT	1413 ± 324[d]	1.4 ± 0.4	0.95 ± 0.14
	3M	1470 ± 716[d]	2.1 ± 0.7	1.06 ± 0.15

[a] Association rate constant determined from slope of line from plot of k_{ass} vs (ligand).
[b] Dissociation rate constant determined from *y* intercept of plot of k_{ass} vs (ligand).
[c] Dissociation equilibrium constant determined from ratio of k_{diss}:k_{ass}.
[d] Mean ± SEM of two or more separate experiments.

to the phosphorylated G-CSFR at Y704 and Y744. Stat3 bound to Y704 phosphododecapeptide with a K_D of 0.703 μM and to Y744 phosphododecapeptide with a K_D of 0.95 μM. To understand the structural basis for Stat3 SH2 recruitment to G-CSFR Y704 and Y744, we performed peptide immunoblot and mirror resonance affinity measurements using G-CSFR-derived dodecapeptides and a series of wild-type and mutated Stat3 proteins. Two models for Stat3 SH2 binding to YxxQ/C-containing ligands were examined initially—each assumed an extended peptide configuration and proposed that the pY residue interacts at one site (pocket 1) and the + 3 Q/C interacts at another site (pocket 2) formed by key residue side chains. Our mutational analysis revealed that while mutations in pocket 1 (K591L and R609L) eliminated binding to Y704 and Y744 phosphododecapeptides, mutation of all the residues proposed to form pocket 2 had, at most, a small effect on binding to these phosphododecapeptides, indicating that pocket 1 is required for binding the pY within these phosphododecapeptides but leaving unresolved the structural basis for specificity of Stat3 SH2 binding to G-CSFR Y704 and Y744 phosphododecapeptides with + 3 Q and C, respectively. Computational analysis using the known structures of EGFR Y1068 phosphopeptide (EpYINQ), which contains a β turn, and Stat3β suggested an alternative model for +Q binding in which the oxygen on the side chain of the pY + 3 Q forms a bond with the amide hydrogen within the peptide backbone of Stat3 at E638. To test this model, we generated recombinant full-length Stat3 protein containing mutation E638P (Stat3-E638P), which eliminated the donor hydrogen. Stat3-E638P demonstrated undetectable binding to Y704 phosphododecapeptide in peptide pull-down and mirror resonance affinity analyses. Coexpression of full-length G-CSFR with either wild-type or mutant Stat3 cDNA constructs in vivo indicated that the side chain of R609 and the amide hydrogen of E638 within the Stat3 SH2 domain make major contributions to Stat3 recruitment and activation by the G-CSFR in vivo, while the side chain of K591 makes a less important contribution to these processes. Thus, our findings support a model of Stat3 SH2 recruitment and activation by G-CSFR at the Y704 site in which binding of Stat3 SH2 occurs through a

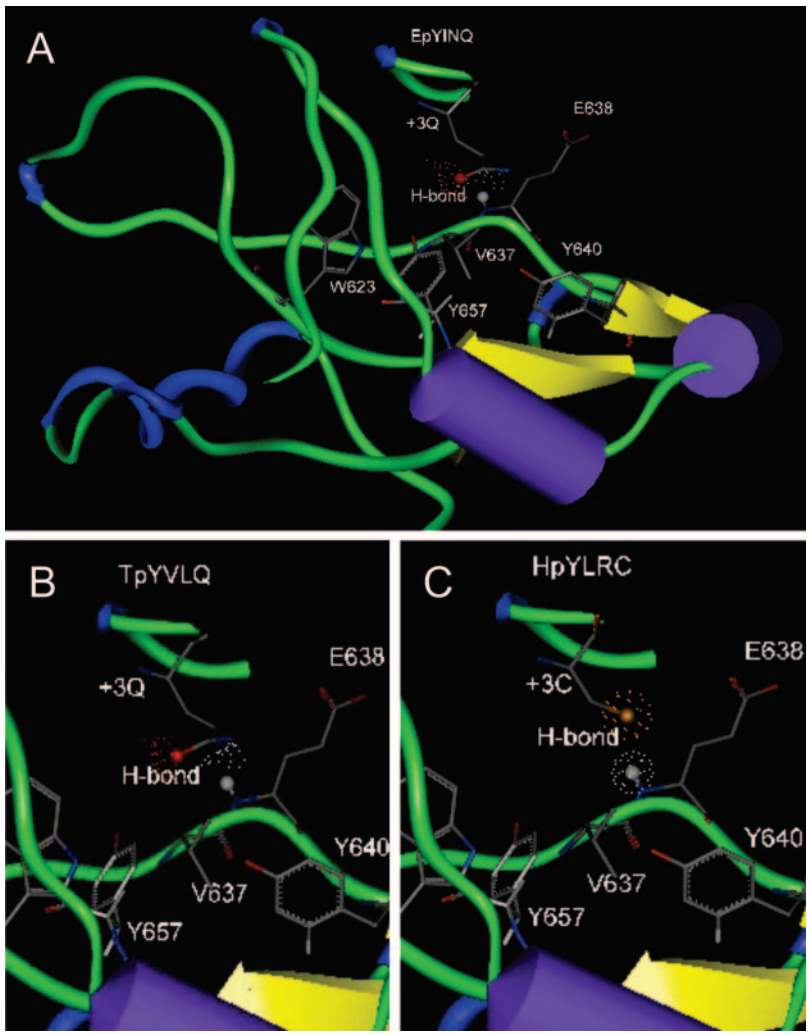

FIGURE 3. Revised model of Stat3 SH2 binding to + 3 Q/C within YxxQ/C-containing phosphopeptide ligands. *A*, Computational modeling using the Biopolymer program in the Insight II environment was used to perform local energy optimization of the interaction of Stat3 SH2 with phosphopeptide ligand EpYINQ (contained within the EGFR and demonstrated to recruit both Stat3 and Grb2) based on the known structures of each. As indicated, the oxygen on the side chain of the pY + 3 Q within the EpYINQ peptide is predicted to form a hydrogen (H) bond with the amide hydrogen at E638 and to make a major contribution to the binding energy. The positions are shown for the side chains of E638, Y640, and Y657 proposed by Chakraborty to form pocket 2 and for the side chain of W623 proposed to force a β turn in the peptide ligand. Models of Stat3 binding to Y704 phosphopentapeptide ligand (*B*) and to Y744 phosphopentapeptide ligand (*C*).

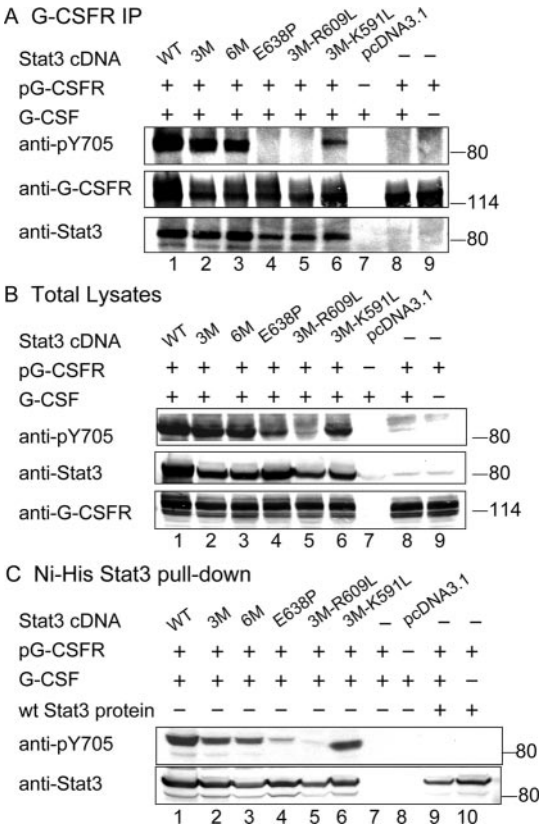

FIGURE 4. Requirement for the side chain of R609 and the amide hydrogen of E638 for Stat3 binding to the G-CSFR and Stat3 phosphorylation on Y705 in vivo. 293T cells were transfected with G-CSFR alone or cotransfected with G-CSFR and either wild-type Stat3 cDNA construct, mutant Stat3 cDNA construct, or empty eukaryotic expression vector (pcDNA3.1) vector as indicated. After 48 h incubation, the cells were stimulated with G-CSF (100 ng/ml) for 15 min as indicated, and the cells were lysed. *A*, Cell lysates were immunoprecipitated with anti-G-CSFR Ab and protein G-agarose (Sigma-Aldrich) at 4°C for 2 h. Immunoprecipitates were separated by SDS-PAGE and immunoblotted for pStat3, total Stat3, and G-CSFR as indicated. *B*, Equal amounts of lysates based on protein content were separated by SDS-PAGE and immunoblotted for pStat3, total Stat3, and G-CSFR as indicated. *C*, Cell lysates were incubated with Ni-NTA agarose (*lanes 1–8*). *Lanes 9* and *10*, Equal amounts of purified Stat3 were mixed with lysates from cells transfected by G-CSFR vector only before incubation with Ni-NTA agarose. Affinity-purified proteins were separated by SDS-PAGE and immunoblotted for pStat3 and total Stat3 as indicated.

critical interaction of its R609 side chain with pY704 followed by or concurrent with the receptor in the regions of these tyrosine forming a β turn, which allows the amide hydrogen of E638 to bind to the + 3 Q (Fig. 1*A*, *bottom panel*). Mutation E638P within Stat3 also eliminated Stat3 binding to G-CSFR Y744 phosphododecapeptide containing + 3 C. As modeled in Fig. 3*C*, the amide hydrogen of E638 is able to form a hydrogen bond with the cysteine sulfur. Cysteine sulfhydryl groups, when they are involved in hydrogen bonds, more commonly serve as hydrogen donors; however, they can serve as hydrogen bond acceptors as in the case of the D169C mutant of thymidine synthase (37).

Stat3 activation by the G-CSFR is thought to occur through two pathways—one that requires G-CSFR Y704 and Y744 (19) and one that does not (6). Review of the results of coexpression studies (Fig. 4*A*) reveals that there is complete elimination of pStat3 bound to the G-CSFR and a >90% reduction in levels of pStat3 in both total cell lysates and His-Stat3 affinity purified from G-CSF-stimulated cells cotransfected with G-CSFR and Stat3-3M-R609L compared with cells cotransfected with G-CSFR and wild-type Stat3. These results suggest that Stat3 recruitment and activation downstream of G-CSF that occurs independently of G-CSFR Y704 and Y744 (6), similar to Stat3 recruitment and activation that is G-CSFR Y704/744 dependent, requires that Stat3 be competent to bind to YxxQ/C-like recruitment sites.

Additional pY peptide motifs proposed to bind Stat3 besides pYxxQ and pYxxC include pY^{705}LKT within Stat3 itself (38) and pY^{743}IRS within the murine G-CSFR (6). Similar to pYxxC, the + 3 aa residue contains a polar side chain each consisting of a hydroxyl group. When substituted for TpY^{704}VLQ in computer-modeled interactions with Stat3 SH2, phosphopentapeptides PpY^{705}LKT and QpY^{743}IRS are capable of forming a hydrogen bond with the E638 amide hydrogen within the Stat3 SH2 domain (data not shown).

SH2 domains are structurally conserved protein modules of ~100 aa residues in length first identified as noncatalytic regions of homology within Src and Fps kinases (39). The structure of 17 SH2 domains have been resolved crystallographically or by nuclear magnetic resonance either in isolation or bound to their pY ligands (reviewed in Ref. 40). The elements of SH2 involved in pY recognition are provided by αA and βB, notably R or K at position αA2 and R at position βB5. In Stat3, the K591 aligns at the αA2 position and R609 at the βB5 position. Our affinity studies demonstrated that binding of Y704 and Y744 phosphododecapeptides by recombinant Stat3 was eliminated when K591L or R609L mutations were introduced in to Stat3, confirming the contribution of the side chains of K591 and R609 to binding pY within the phosphopeptide ligand in vitro. However, our coexpression studies indicated that elimination of the K591 but not the side chain of R609 was fully compensated for in vivo, indicating that K591 is not as critical as R609 to binding in vivo. This result is consistent with a recent energetics analysis that predicted no contribution of the side chain of residue αA2 within several SH2 domains (Jak1, Jak2, Jak3, Tyk2, SHPTP2-C, and Cbl) to recognition of the pY residue (40).

The amino acids C-terminal to pY that form the basis for specificity in SH2-pY peptide especially depend on the nature of residue + 2 or + 3 relative to the pY residue (21, 22). Phosphopeptides with specificity at + 3 tend to interact in an extended conformation with the surface of the SH2 domain. The prototype of this interaction is that between the Src-family SH2 domains and peptides containing the optimal pYEEI motif (41), which resembles a two-pronged plug (the peptide) engaging a two-holed socket (the SH2 domain). Phosphopeptides with specificity at + 2 adopt a β turn conformation. With the exception of Stat3 SH2 proposed in this article, the only known example of this interaction is that between the Grb2 SH2 domain and peptides containing the Grb2 consensus motif pYxNx. Review of the model of Stat3 SH2 bound to peptide EpYINQ (Fig. 3*A*) reveals that W623 occupies a position in Stat3 SH2 that may serve to block binding of YxxQ peptide in the extended conformation and force a β turn similar to W121 in Grb2. Of note, two groups have recently demonstrated preferential binding of Stat3 to phosphopeptide ligands with P in the + 2 position (42, 43); P in the + 2 position favors formation of β turns (44). Taken together, our results identify the structural basis of the Stat3 SH2 pY peptide ligand preference for those peptides having amino acid residues with polar side chains—Q, C, T, and S—at the + 3 position. In addition, our studies identify an additional peptide requirement for binding by Stat3 SH2, i.e., the ability of the peptide to assume a β turn to allow the + 3 residue hydrogen bond acceptor (oxygen or sulfur) to form a bond with amide hydrogen of E638 within Stat3. This requirement for the pY

peptide ligand to form a β turn may not be unique to Stat3 but may be shared by other members of the STAT protein family. Stat1, Stat2, Stat4, Stat5A, and Stat5B each have W at an analogous position to W623 in Stat3 (26). Similar to W623 in Stat3, the bulky side chain of W may prevent their respective pY peptide ligands from binding in an extended conformation. Indeed, the recently published crystal structure of Stat1 bound to its pY ligand docking site within the IFN-γR reveals that the pY ligand, when bound by the Stat2 SH2 domain, is not in an extended configuration but rather has a sharp bend at the pY + 1 position (45).

Imatinib mesylate (Gleevec) and its derivatives (46) that target PTK, most notably Bcr-Abl, have been heralded as leading the way toward a new age of cancer therapy marked by structure-assisted drug design (47). Structure-based strategies also are being pursued by pharmaceutical firms and other groups to develop peptidomimetics that target SH2-pY interactions based on the known structures of these interactions for treatment of cancer and other diseases (36, 48–50).

Flt3 internal tandem duplications are found in 30–35% of AML patients and have been associated with a poor prognosis (reviewed in Ref. 51). Recently, AML patients whose cells contain Flt3 internal tandem duplications have been shown to aberrantly activate Stat3 following stimulation with G-CSFR, a finding associated with frequent relapse following induction chemotherapy (10). Constitutive Stat3 activation had been demonstrated previously in 44% of AML patient samples and was associated with decreased disease-free survival (52). Targeting of Stat3 using antisense strategies, dominant-negative constructs, and oligonucleotides that destabilize Stat3 dimers have been shown experimentally to induce apoptosis and reduce tumor cell growth in a variety of human cancers, including large granular lymphocytic leukemia (53), myeloma (54), breast (55, 56), prostate (56, 57), and squamous cell carcinoma of the head and neck (58, 59). Our results suggest a strategy that can be pursued to develop peptidomimetics or small molecules that target Stat3 recruitment and activation in tumor cells systems with aberrant Stat3 activation such as AML with Flt3 internal duplications. Given the unique combination of structural features that characterize Stat3 SH2 binding to preferred pY peptide ligands, such targeting would be predicted to be highly specific for Stat3 recruitment and activation not only by the G-CSFR but also by other receptors and proteins containing the pYxxQ/C/T consensus binding motif for Stat3 SH2. Also, given the findings of Lee et al. (60) using targeted deletion of Stat3 in early myeloid progenitor cells that Stat3 activation downstream of G-CSF may in fact be a negative regulator of normal granulopoiesis (60), transient targeting of Stat3 would not be expected to be complicated by myelosuppression.

Acknowledgments

We thank Dr. Richard G. Cook (Baylor College of Medicine) for assistance in the mirror resonance imaging studies.

Disclosures

The authors have no financial conflict of interest.

References

1. Tian, S. S., P. Lamb, H. M. Seidel, R. B. Stein, and J. Rosen. 1994. Rapid activation of the STAT3 transcription factor by granulocyte colony-stimulating factor. *Blood* 84: 1760–1764.
2. Tweardy, D. J., T. M. Wright, S. F. Ziegler, H. Baumann, A. Chakraborty, S. M. White, K. F. Dyer, and K. A. Rubin. 1995. Granulocyte colony-stimulating factor rapidly activates a distinct STAT-like protein in normal myeloid cells. *Blood* 86: 4409–4416.
3. Chakraborty, A., S. M. White, T. S. Schaefer, E. D. Ball, K. F. Dyer, and D. J. Tweardy. 1996. Granulocyte colony-stimulating factor activation of Stat3α and Stat3β in immature normal and leukemic human myeloid cells. *Blood* 88: 2442–2449.
4. Shimozaki, K., K. Nakajima, T. Hirano, and S. Nagata. 1997. Involvement of STAT3 in the granulocyte colony-stimulating factor-induced differentiation of myeloid cells. *J. Biol. Chem.* 272: 25184–25189.
5. Chakraborty, A., and D. J. Tweardy. 1998. Stat3 and G-CSF-induced myeloid differentiation. *Leuk. Lymphoma* 30: 433–442.
6. Ward, A. C., L. Smith, J. P. de Koning, Y. van Aesch, and I. P. Touw. 1999. Multiple signals mediate proliferation, differentiation, and survival from the granulocyte colony-stimulating factor receptor in myeloid 32D cells. *J. Biol. Chem.* 274: 14956–14962.
7. de Koning, J. P., A. A. Soede-Bobok, A. C. Ward, A. M. Schelen, C. Antonissen, D. van Leeuwen, B. Lowenberg, and I. P. Touw. 2000. STAT3-mediated differentiation and survival and of myeloid cells in response to granulocyte colony-stimulating factor: role for the cyclin- dependent kinase inhibitor $p27^{Kip1}$. *Oncogene* 19: 3290–3298.
8. McLemore, M. L., S. Grewal, F. Liu, A. Archambault, J. Poursine-Laurent, J. Haug, and D. C. Link. 2001. STAT-3 activation is required for normal G-CSF-dependent proliferation and granulocytic differentiation. *Immunity* 14: 193–204.
9. Maun, N. A., P. Gaines, A. Khanna-Gupta, T. Zibello, L. Enriquez, L. Goldberg, and N. Berliner. 2004. G-CSF signaling can differentiate promyelocytes expressing a defective retinoic acid receptor: evidence for divergent pathways regulating neutrophil differentiation. *Blood* 103: 1693–1701.
10. Irish, J. M., R. Hovland, P. O. Krutzik, O. D. Perez, O. Bruserud, B. T. Gjertsen, and G. P. Nolan. 2004. Single cell profiling of potentiated phospho-protein networks in cancer cells. *Cell* 118: 217–228.
11. Taniguchi, T. 1995. Cytokine signaling through nonreceptor protein tyrosine kinases. *Science* 268: 251–255.
12. Nicholson, S. E., A. C. Oates, A. G. Harpur, A. Ziemiecki, A. F. Wilks, and J. E. Layton. 1994. Tyrosine kinase JAK1 is associated with the granulocyte-colony-stimulating factor receptor and both become tyrosine-phosphorylated after receptor activation. *Proc. Natl. Acad. Sci. USA* 91: 2985–2988.
13. Shimoda, K., H. Iwasaki, S. Okamura, Y. Ohno, A. Kubota, F. Arima, T. Otsuka, and Y. Niho. 1994. G-CSF induces tyrosine phosphorylation of the JAK2 protein in the human myeloid G-CSF responsive and proliferative cells, but not in mature neutrophils. *Biochem. Biophys. Res. Commun.* 203: 922–928.
14. Nicholson, S. E., U. Novak, S. F. Ziegler, and J. E. Layton. 1995. District regions of the granulocyte colony-stimulating factor receptor are required for tyrosine phosphorylation of the signaling molecules JAK2, Stat3, and p42, p44MAPK. *Blood* 86: 3698–3704.
15. de Koning, J. P., A. M. Schelen, F. Dong, C. van Buitenen, B. M. Burgering, J. L. Bos, B. Lowenberg, and I. P. Touw. 1996. Specific involvement of tyrosine 764 of human granulocyte colony-stimulating factor receptor in signal transduction mediated by p145/Shc/GRB2 or p90/GRB2 complexes. *Blood* 87: 132–140.
16. Kendrick, T. S., R. J. Lipscombe, O. Rausch, S. E. Nicholson, J. E. Layton, L. C. Goldie-Cregan, and M. A. Bogoyevitch. 2004. Contribution of the membrane-distal tyrosine in intracellular signaling by the granulocyte colony-stimulating factor receptor. *J. Biol. Chem.* 279: 326–340.
17. Hunter, M. G., and B. R. Avalos. 1998. Phosphatidylinositol 3′-kinase and SH2-containing inositol phosphatase (SHIP) are recruited by distinct positive and negative growth-regulatory domains in the granulocyte colony-stimulating factor receptor. *J. Immunol.* 160: 4979–4987.
18. Hortner, M., U. Nielsch, L. M. Mayr, J. A. Johnston, P. C. Heinrich, and S. Haan. 2002. Suppressor of cytokine signaling-3 is recruited to the activated granulocyte-colony stimulating factor receptor and modulates its signal transduction. *J. Immunol.* 169: 1219–1227.
19. Chakraborty, A., K. F. Dyer, M. Cascio, T. A. Mietzner, and D. J. Tweardy. 1999. Identification of a novel Stat3 recruitment and activation motif within the granulocyte colony-stimulating factor receptor. *Blood* 93: 15–24.
20. Ward, A. C., Y. M. van Aesch, A. M. Schelen, and I. P. Touw. 1999. Defective internalization and sustained activation of truncated granulocyte colony-stimulating factor receptor found in severe congenital neutropenia/acute myeloid leukemia. *Blood* 93: 447–458.
21. Songyang, Z., S. E. Shoelson, M. Chaudhuri, G. Gish, T. Pawson, W. G. Haser, F. King, T. Roberts, S. Ratnofsky, R. J. Lechleider, et al. 1993. SH2 domains recognize specific phosphopeptide sequences. *Cell* 72: 767–778.
22. Cantley, L. C., and Z. Songyang. 1994. Specificity in recognition of phosphopeptides by src-homology 2 domains. *J. Cell Sci. Suppl.* 18: 121–126.
23. Stahl, N., T. J. Farruggella, T. G. Boulton, Z. Zhong, J. E. Darnell, Jr., and G. D. Yancopoulos. 1995. Choice of STATs and other substrates specified by modular tyrosine-based motifs in cytokine receptors. *Science* 267: 1349–1353.
24. Weber-Nordt, R. M., J. K. Riley, A. C. Greenlund, K. W. Moore, J. E. Darnell, and R. D. Schreiber. 1996. Stat3 recruitment by two distinct ligand-induced, tyrosine-phosphorylated docking sites in the interleukin-10 receptor intracellular domain. *J. Biol. Chem.* 271: 27954–27961.
25. Rahuel, J., B. Gay, D. Erdmann, A. Strauss, C. Garcia-Echeverria, P. Furet, G. Caravatti, H. Fretz, J. Schoepfer, and M. G. Grutter. 1996. Structural basis for specificity of Grb2-SH2 revealed by a novel ligand binding mode. *Nat. Struct. Biol.* 3: 586–589.
26. Becker, S., B. Groner, and C. W. Muller. 1998. Three-dimensional structure of the Stat3β homodimer bound to DNA. *Nature* 394: 145–151.
27. Hemmann, U., C. Gerhartz, B. Heesel, J. Sasse, G. Kurapkat, J. Grotzinger, A. Wollmer, Z. Zhong, J. E. Darnell, Jr., L. Graeve, et al. 1996. Differential activation of acute phase response factor/Stat3 and Stat1 via the cytoplasmic domain of the interleukin 6 signal transducer gp130. II. Src homology SH2 domains define the specificity of stat factor activation. *J. Biol. Chem.* 271: 12999–13007.
28. Caldenhoven, E., D. T. B. van Dijk, R. Solari, J. Armstrong, J. A. M. Raaijmakers, J. W. J. Lammers, L. Koenderman, and R. P. de Groot. 1996. STAT3β, a splice

variant of transcription factor STAT3, is a dominant negative regulator of transcription. *J. Biol. Chem.* 271: 13221–13227.
29. Shao, H., H. Y. Cheng, R. G. Cook, and D. J. Tweardy. 2003. Identification and characterization of signal transducer and activator of transcription 3 recruitment sites within the epidermal growth factor receptor. *Cancer Res.* 63: 3923–3930.
30. Schuenke, K. W., R. G. Cook, and R. R. Rich. 1998. Binding specificity of a class II-restricted hepatitis B epitope by DR molecules from responder and nonresponder vaccine recipients. *Hum. Immunol.* 59: 783–793.
31. Leatherbarrow, R. J. 1998. *GraFit Version 4.* Erithacus Software Ltd., Staines.
32. Ziegler, S. F., T. Davis, J. A. Schneringer, T. L. Franklin, T. W. Tough, M. Teepe, A. Larsen, D. E. Williams, and C. A. Smith. 1991. Alternative forms of the human G-CSF receptor function in growth signal transduction. [Published erratum appears in *1992 New Biol. 4: 172.*] *New Biol.* 3: 1242–1248.
33. van de Geijn, G. J., J. Gits, and I. P. Touw. 2004. Distinct activities of suppressor of cytokine signaling (SOCS) proteins and involvement of the SOCS box in controlling G-CSF signaling. *J. Leukocyte Biol.* 76: 237–244.
34. Nicholson, S. E., R. Starr, U. Novak, D. J. Hilton, and J. E. Layton. 1996. Tyrosine residues in the granulocyte colony-stimulating factor (G-CSF) receptor mediate G-CSF-induced differentiation of murine myeloid leukemic (M1) cells. *J. Biol. Chem.* 271: 26947–26953.
35. Shao, H., X. Xu, M. A. Mastrangelo, N. Jing, R. G. Cook, G. B. Legge, and D. J. Tweardy. 2004. Structural requirements for signal transducer and activator of transcription 3 binding to phosphotyrosine ligands containing the YXXQ motif. *J. Biol. Chem.* 279: 18967–18973.
36. Rahuel, J., C. Garcia-Echeverria, P. Furet, A. Strauss, G. Caravatti, H. Fretz, J. Schoepfer, and B. Gay. 1998. Structural basis for the high affinity of amino-aromatic SH2 phosphopeptide ligands. *J. Mol. Biol.* 279: 1013–1022.
37. Birdsall, D. L., J. Finer-Moore, and R. M. Stroud. 2003. The only active mutant of thymidylate synthase D169, a residue far from the site of methyl transfer, demonstrates the exquisite nature of enzyme specificity. *Protein Eng.* 16: 229–240.
38. Turkson, J., D. Ryan, J. S. Kim, Y. Zhang, Z. Chen, E. Haura, A. Laudano, S. Sebti, A. D. Hamilton, and R. Jove. 2001. Phosphotyrosyl peptides block Stat3-mediated DNA binding activity, gene regulation, and cell transformation. *J. Biol. Chem.* 276: 45443–45455.
39. Sadowski, I., J. C. Stone, and T. Pawson. 1986. A noncatalytic domain conserved among cytoplasmic protein-tyrosine kinases modifies the kinase function and transforming activity of Fujinami sarcoma virus P130gag-fps. *Mol. Cell. Biol.* 6: 4396–4408.
40. Sheinerman, F. B., B. Al-Lazikani, and B. Honig. 2003. Sequence, structure and energetic determinants of phosphopeptide selectivity of SH2 domains. *J. Mol. Biol.* 334: 823–841.
41. Waksman, G., S. E. Shoelson, N. Pant, D. Cowburn, and J. Kuriyan. 1993. Binding of a high affinity phosphotyrosyl peptide to the Src SH2 domain: crystal structures of the complexed and peptide-free forms. *Cell* 72: 779–790.
42. Ren, Z., L. A. Cabell, T. S. Schaefer, and J. S. McMurray. 2003. Identification of a high-affinity phosphopeptide inhibitor of stat3. *Bioorg. Med. Chem. Lett.* 13: 633–636.
43. Wiederkehr-Adam, M., P. Ernst, K. Muller, E. Bieck, F. O. Gombert, J. Ottl, P. Graff, F. Grossmuller, and M. H. Heim. 2003. Characterization of phosphopeptide motifs specific for the Src homology 2 domains of signal transducer and activator of transcription 1 (STAT1) and STAT3. *J. Biol. Chem.* 278: 16117–16128.
44. Guruprasad, K., and S. Rajkumar. 2000. β- and γ-turns in proteins revisited: a new set of amino acid turn-type dependent positional preferences and potentials. *J. Biosci.* 25: 143–156.
45. Mao, X., Z. Ren, G. N. Parker, H. Sondermann, M. A. Pastorello, W. Wang, J. S. McMurray, B. Demeler, J. E. Darnell, Jr., and X. Chen. 2005. Structural bases of unphosphorylated STAT1 association and receptor binding. *Mol. Cell* 17: 761–771.
46. Shah, N. P., C. Tran, F. Y. Lee, P. Chen, D. Norris, and C. L. Sawyers. 2004. Overriding imatinib resistance with a novel ABL kinase inhibitor. *Science* 305: 399–401.
47. Noble, M. E., J. A. Endicott, and L. N. Johnson. 2004. Protein kinase inhibitors: insights into drug design from structure. *Science* 303: 1800–1805.
48. Li, P., M. Zhang, Y. Q. Long, M. L. Peach, H. Liu, D. Yang, M. Nicklaus, and P. P. Roller. 2003. Potent Grb2-SH2 domain antagonists not relying on phosphotyrosine mimics. *Bioorg. Med. Chem. Lett.* 13: 2173–2177.
49. Kawahata, N., M. G. Yang, G. P. Luke, W. C. Shakespeare, R. Sundaramoorthi, Y. Wang, D. Johnson, T. Merry, S. Violette, W. Guan, et al. 2001. A novel phosphotyrosine mimetic 4′-carboxymethyloxy-3′-phosphonophenylalanine (Cpp): exploitation in the design of nonpeptide inhibitors of pp60(Src) SH2 domain. *Bioorg. Med. Chem. Lett.* 11: 2319–2323.
50. Sawyer, T. K., R. S. Bohacek, D. C. Dalgarno, C. J. Eyermann, N. Kawahata, C. A. Metcalf, 3rd, W. C. Shakespeare, R. Sundaramoorthi, Y. Wang, and M. G. Yang. 2002. SRC homology-2 inhibitors: peptidomimetic and nonpeptide. *Mini Rev. Med. Chem.* 2: 475–488.
51. Gilliland, D. G., and J. D. Griffin. 2002. Role of FLT3 in leukemia. *Curr. Opin. Hematol.* 9: 274–281.
52. Benekli, M., Z. Xia, K. A. Donohue, L. A. Ford, L. A. Pixley, M. R. Baer, H. Baumann, and M. Wetzler. 2002. Constitutive activity of signal transducer and activator of transcription 3 protein in acute myeloid leukemia blasts is associated with short disease-free survival. *Blood* 99: 252–257.
53. Epling-Burnette, P. K., J. H. Liu, R. Catlett-Falcone, J. Turkson, M. Oshiro, R. Kothapalli, Y. Li, J. M. Wang, H. F. Yang-Yen, J. Karras, et al. 2001. Inhibition of STAT3 signaling leads to apoptosis of leukemic large granular lymphocytes and decreased Mcl-1 expression. *J. Clin. Invest.* 107: 351–362.
54. Catlett-Falcone, R., T. H. Landowski, M. M. Oshiro, J. Turkson, A. Levitzki, R. Savino, G. Ciliberto, L. Moscinski, J. L. Fernandez-Luna, G. Nunez, et al. 1999. Constitutive activation of Stat3 signaling confers resistance to apoptosis in human U266 myeloma cells. *Immunity* 10: 105–115.
55. Garcia, R., T. L. Bowman, G. Niu, H. Yu, S. Minton, C. A. Muro-Cacho, C. E. Cox, R. Falcone, R. Fairclough, S. Parsons, et al. 2001. Constitutive activation of Stat3 by the Src and JAK tyrosine kinases participates in growth regulation of human breast carcinoma cells. *Oncogene* 20: 2499–2513.
56. Jing, N., Y. Li, W. Xiong, W. Sha, L. Jing, and D. J. Tweardy. 2004. G-quartet oligonucleotides: a new class of signal transducer and activator of transcription 3 inhibitors that suppresses growth of prostate and breast tumors through induction of apoptosis. *Cancer Res.* 64: 6603–6609.
57. Mora, L. B., R. Buettner, J. Seigne, J. Diaz, N. Ahmad, R. Garcia, T. Bowman, R. Falcone, R. Fairclough, A. Cantor, et al. 2002. Constitutive activation of Stat3 in human prostate tumors and cell lines: direct inhibition of Stat3 signaling induces apoptosis of prostate cancer cells. *Cancer Res.* 62: 6659–6666.
58. Grandis, J. R., S. D. Drenning, A. Chakraborty, M. Y. Zhou, Q. Zeng, A. S. Pitt, and D. J. Tweardy. 1998. Requirement of Stat3 but not Stat1 activation for epidermal growth factor receptor-mediated cell growth In vitro. *J. Clin. Invest.* 102: 1385–1392.
59. Grandis, J. R., S. D. Drenning, Q. Zeng, S. C. Watkins, M. F. Melhem, S. Endo, D. E. Johnson, L. Huang, Y. He, and J. D. Kim. 2000. Constitutive activation of Stat3 signaling abrogates apoptosis in squamous cell carcinogenesis in vivo. *Proc. Natl. Acad. Sci. USA* 97: 4227–4232.
60. Lee, C. K., R. Raz, R. Gimeno, R. Gertner, B. Wistinghausen, K. Takeshita, R. A. DePinho, and D. E. Levy. 2002. STAT3 is a negative regulator of granulopoiesis but is not required for G-CSF-dependent differentiation. *Immunity* 17: 63–72.